

# **Enhancement of Impact-Synchronous Modal analysis (ISMA) with number of averages**

**A.G.A. RAHMAN**

*Faculty of Mechanical Engineering, University Malaysia Pahang, 26600 Pekan, Pahang Darul Makmur, MALAYSIA*

**Z. ISMAIL**

*Civil Engineering Department, Faculty of Engineering, University of Malaya, 50603 Kuala Lumpur, MALAYSIA*

**S. NOROOZI**

*School of Design, Engineering and Computing, Bournemouth University (Talbot Campus), Poole, Dorset, BH12 5BB, UK*

**Z.C. ONG**

*Mechanical Engineering Department, Faculty of Engineering, University of Malaya, 50603 Kuala Lumpur, MALAYSIA (zhichao83@gmail.com)*

## **ABSTRACT**

*A new method, namely Impact-Synchronous Modal Analysis (ISMA) utilizing the modal extraction technique commonly used in Experimental Modal Analysis (EMA) performed in the presence of the ambient forces, is proposed. In ISMA, the extraction is performed while the machine is running, utilized Impact-Synchronous Time Averaging (ISTA) prior to performing the Fast Fourier Transform (FFT). The number of averaging had a very important effect when applying ISMA on structures with dominant periodic responses of cyclic loads and ambient excitation. With sufficient number of impacts, all the unaccounted forces were diminished, leaving only the response due to the impacts. This study demonstrated the effectiveness of averages taken in the determination of dynamic characteristics of a machine while in different rotating speeds. At low operating speeds which coincided with the lower natural modes, ISMA with high number of impacts determined the*

*dynamic characteristics of the system successfully. Meanwhile, at operating speeds which were away from any natural modes, ISMA with moderate number of averages taken was sufficient enough to extract the modal parameters. Finally for high speed machines, ISMA with high number of impacts taken has limitations in extracting natural modes close to the operating speed.*

**KEYWORDS:** *Experimental Modal Analysis, Impact-Synchronous Modal Analysis, Impact-Synchronous Time Averaging, Modal Assurance Criterion, Averages*

## **1. INTRODUCTION**

Experimental Modal analysis (EMA), requires the system to be in complete ‘shutdown’ mode. In other words, there should be no unaccounted excitation force induced into the system. Measurable impact or random forces are used to excite the system. The responses of the system are auto-correlated and cross-correlated with the measured inputs. The correlation functions are transformed to frequency domain to obtain the transfer functions. This procedure is repeated at a discrete set of geometrical positions sufficient enough to describe the structure. Various curve-fitting algorithms (Maia and Silva, 1997; Richardson and Formenti, 1982; Richardson and Formenti, 1985; Shih et al., 1988; Avitabile, 2011) are then used to extract the three modal parameters. In applications, the extracted modal parameters from EMA have been widely used to detect damage on beams and beam-like structures as well as rotor systems (Fayyadh et al., 2011; Ismail and Ong, 2012; Ismail, 2012; Ismail et al., 2011; Ong et al., 2012)

A method called Operational Modal Analysis (OMA) has been introduced and various studies have been conducted in order to perform modal analysis while the machines are running. Modal parameters

identification techniques have been developed using multi-output data only (Lardies and Larbi, 2001b; Lardies and Larbi, 2001a). In OMA, structural modal parameters can be computed without knowing the input excitation to the system. It is therefore a valuable tool to analyze structures subjected to excitation generated by their own operation. Presently, operational modal analysis procedures are limited to the case when excitation to the system is white stationary noise (Mohanty and Rixen, 2004). There are other different ways to identify modal parameters in such a case. One approach called the natural excitation technique (NExT) (James et al., 1995) consists of computing correlations between the response signals and observes that they can be compared to impulse responses of the system. Hence, the output correlation functions can be processed as the impulse response functions of the system to extract modal parameters. Standard time-domain identification techniques such as the least squares complex exponential method (LSCE) (Brown et al., 1985), the eigenvalue realization algorithm (ERA) (Juang and Pappa, 1985) and the Ibrahim Time Domain method (ITD) (Ibrahim and Mikulcik, 1973; Ibrahim and Mikulcik, 1976; Ibrahim and Mikulcik, 1977; Pappa and Ibrahim, 1981) can be applied as identification techniques.

In practical situations where the system cannot have a complete ‘shutdown’ or the structure is too large to response to ‘artificial’ excitation, OMA is sought. Here, the operating forces coming from the structure cyclic loads or ambient forces are used as the exciters. As these quantities cannot be measured, OMA utilised only information from the measurable responses (multi-output data). Some algorithms are used to extract the three modal parameters (Zhang et al., 2001; Brincker et al., 2000; Schwarz and Richardson, 2001; Schwarz and Richardson, 2007; Whelan et al., 2011). Researchers combined OMA with correction technique of spectrum analysis (CTSA) (Kang et al., 2000; Ming and Kang, 1996), harmonic wavelet filtering

(HWF), random decrement technique (RDT) and Hilbert transform (HT) method to obtain these parameters (Qi et al., 2008).

Meanwhile, there are some existing software which come with OMA option. OMA may be used instead of Classical Modal Analysis for modal identification under actual operating conditions and in situations where it is difficult or impossible to control an artificial excitation of the structure. The main advantage of OMA is the measured responses are used for modal identification of structures under actual operation without the excitation from hammer and shaker. Finally, the measured response is representative of the actual operating conditions of the structure.

Various researchers have been conducting OMA to perform modal analysis while the structures and systems are running. OMA holds certain advantages over EMA for its practicality and easiness to carry out. Also, it performs the analysis while the system is running and the measured responses are representative of the actual operating conditions of the structure. However, the lack of knowledge of the input forces does affect the parameters extracted. For example, mode shapes obtained from OMA cannot be normalised accurately, subsequently affecting the mathematical models.

Over the years, in an effort to improve the estimation accuracy in OMA and EMA, the focus has been mainly to develop modal identification algorithms. Relatively less effort is made on the digital signal processing aspects, especially upstream of the collected data. Impact-Synchronous Modal Analysis or ISMA has advantages over the OMA and EMA combined. It carries out the analysis while the system is running and

at the same time is able to provide the actual input forces in the transfer functions, hence, allowing for better modal extractions.

In Impact-Synchronous Modal Analysis (ISMA), where it is performed while machine is in running mode, all the responses contributed by the unaccounted forces are filtered out in the time domain, leaving only the response due to the impact hammer. This is achieved by utilizing the Impact-Synchronous Time Averaging (ISTA) (Rahman et al., 2011a) prior to performing the Fast Fourier Transform (FFT). Apart from this, modal parameters extraction follows the EMA procedures.

The limitation of ISMA is in its application on large structures where the impact response may be too small as compared to the operating cyclic loads. Excessive impacts may result in non-linearity (Rahman et al., 2011b). It is noted that responses from unaccounted forces that contain even the same frequency as that contained in the impulse response is diminished if the phase is not consistent with the impact signature only if sufficient number of impacts is taken (Rahman et al., 2011b).

In this paper, ISMA was further investigated in order to improve this modal analysis technique. The number of impacts applied on the structures was studied at different operating cyclic load conditions. Effect of averaging numbers was noted to be very important parameter when applying ISMA on structures with dominant periodic responses of cyclic loads and ambient excitation. With sufficient number of impacts, all the unaccounted forces were diminished, leaving only the response due to the impacts.

## 2. MATHEMATICAL BACKGROUND

### 2.1 IMPACT-SYNCHRONOUS TIME AVERAGING

Impact-Synchronous Time Averaging incorporates the time synchronous averaging technique to rapidly improve the signal to noise ratio of the response obtained while the machine is in operating mode. In Impact-Synchronous Time Averaging, block averaging is performed on the time block of both the force and response. Each time block is initiated by the impulse generated from the force trace of the impact hammer. The periodic responses of cyclic loads and ambient excitations are no more in the same phase position for every time block acquired. Equation (1) shows that averaging process of repetitive impact will slowly diminish these components hence leaving behind only the structure impulse responses which are synchronous to the repetitive impact force.

$$y(t) = \frac{1}{N} \sum_{r=0}^{N-1} x(t + rT_o) \quad (1)$$

where  $y(t)$  is the averaged vibration signal in time domain,  $N$  is the number of impacts,  $x(t)$  is the vibration signal in time domain, and  $T_o$  is the time interval between impacts.

The averaged time block of impulse responses is auto and cross spectrum with the averaged time block of impact signatures to generate the transfer function (Rahman et al., 2011a).

## 2.2 Modal Assurance Criterion (MAC)

Modal Assurance Criterion (MAC) is a method for quantitatively comparing a pair of shapes, and it is computed between two complex shape vectors  $\{X\}$ ,  $\{Y\}$  using the following formula (Rahman et al., 2011b; Allemang, 2003),

$$\text{MAC}(\{X\}, \{Y\}) = \frac{|\{X\}^T \cdot \{Y\}|^2}{(\{X\}^T \cdot \{X\}) \cdot (\{Y\}^T \cdot \{Y\})} \quad (2)$$

MAC values range between 0 and 1, and should be interpreted as follows

- MAC = 1.0 means the two mode shapes are identical.
- MAC > 0.9 means the two mode shapes are similar.
- MAC < 0.9 means the two mode shapes are different.

In this study, MAC was used as a quantitative approach to show the correlation of mode shape vectors between EMA and ISMA. Mode shape vectors obtained using EMA during non-rotating condition were used as a benchmark. Mode shape vectors obtained using ISMA during operating conditions were compared with the benchmark and the consistency of the mode shapes were shown in MAC values.

## 3. MEASUREMENT PROCEDURES AND INSTRUMENTATION

A test rig consisted of a motor coupled to rotor shaft system as displayed in Figure 1. It was used in the laboratory to study the effect of impacts numbers in ISMA at different operating conditions.

The instrumentation and procedures used in ISMA was the same as in EMA. The only difference was that the averaging techniques allowed the procedure to be carried while the machine was running.

Rahman et al. (Rahman et al., 2011a; Rahman et al., 2011b) explained the complete experimental procedures of ISMA. Data were obtained by using a data acquisition system together with an impact hammer and tri-axial accelerometer. Five averages or impacts were made using EMA when the system is not running. In ISMA, the system was allowed to operate at three different speeds with averages up to 250 impacts taken. The signals were processed by the virtual instruments to generate the frequency response functions and coherence functions. The modal extraction techniques applied to EMA could also be applied in ISMA. Figure 2 shows a three-dimensional structural model of the test rig which was drawn in coordinate points and connected by straight lines using a modal analysis software called ME'scope. This model was used to display the mode shapes of the rig from the acquired data. In addition, the software performed post-processing of the acquired data and curve-fitting for the extraction of modal frequency, modal damping and modal shape. Modal damping,  $2\sigma$  is approximately equal to the width of the resonance peak at 70.7 % of the FRF peak magnitude value, which is the same as half of the peak magnitude value squared. Hence,  $2\sigma$  is the width at the half power point of a resonance peak. Damping was calculated in term of decay rate,  $\sigma$  which is originally in rad/s. After conversion, it is in Hertz. ME'scope also calculated the MAC value for consistency of mode shape vectors between EMA and ISMA.

#### **4. RESULTS AND DISCUSSION**

Experimental modal analysis (EMA) was performed on the test rig while it is in static condition and the first three modes were extracted. Modal parameters of the first three modes are as tabulated in Table 1. Different numbers of averages were applied in order to study their effect in Impact-Synchronous Modal Analysis (ISMA) at three running conditions. Number averages of 5, 25, 50, 100, 150, 200 and 250 were used

at three different running speeds, i.e. 10 Hz, 20 Hz and 30 Hz. These three operating speeds could be categorised into three different conditions. The effects of these three speed conditions in ISMA as below were studied. At 10Hz, rotational force is low and it coincides with a natural mode. Hence, higher vibration generated. At 20Hz, rotational force increased and it sits in between two natural modes. At 30Hz, running speed component is not coincided with any natural modes. High vibration generated purely due to rotational force. The results obtained from ISMA at different speeds and numbers of averages were then compared with results obtained from EMA. Subsequently, Modal Assurance Criterion (MAC) value is computed to measure consistency of modal vectors obtained from EMA and ISMA. It was noticed that number of averages is an important parameter in ISMA to filter out signatures of non-synchronous components such as cyclic loads and ambient excitations.

First natural mode of 9.92 Hz was observed in EMA's results. At 10 Hz, the operating speed coincided with this first natural mode. This is classified as resonance situation and the operating cyclic load is dominant. At low impact numbers, from the averages of 5 to 25, it was observed that the modal parameters using ISMA were not as consistent when compared to EMA. Lower MAC values also indicate that there are little correlation of eigenvectors or mode shapes between EMA and ISMA. The natural mode was covered by the dominant cyclic load at 10 Hz. By increasing the impact numbers, all responses contributed by unaccounted forces were filtered out, leaving only the structure's response to impulses as the periodic responses of cyclic loads and ambient excitations in different phase position for every impact applied. The results are as tabulated in Table 2. MAC value from the averages of 100 to 250 shows that consistency of the modal vector between EMA and ISMA is established. The MAC values range from 0.951 to 0.957.

Second and third modes of 15.6 Hz and 24.9 Hz are far from the operating speed of 10 Hz. The effect of cyclic load on these two modes is not dominant as compared to the first mode. Table 3 shows that the modal parameters of second mode which were extracted from ISMA are consistent and close to the results from EMA at number of averages ranging from 5 to 250. Stable and high MAC values above 0.9 at low number of impacts such as 5 to 25 averages show that effects of cyclic loads and ambient excitation at these two modes are minimal. Thus, good correlation of modal parameters of second mode between EMA and ISMA has been achieved.

The third mode shape at low averages shows little correlation, with MAC value of only 0.784. MAC value increased with number of averages and recorded a value of 0.871 at 250 averages. The results are tabulated in Table 4. MAC value below 0.9 in the third mode is due to the sensitivity of this mode to excitation in the vertical direction (Z-axis). The third mode is not dominant even in static condition. The natural peak is covered by other natural modes. When the test rig was in operating condition, this mode was hardly excited because it was covered by the other modes as well as the ambient excitations.

At low operating speeds with lower natural modes, increasing number of averages in ISMA could determine the dynamic characteristics of the system, and the results obtained are comparable and well correlated with the benchmarked EMA.

At 20Hz, first mode is far away from this operating speed. It was observed that the extracted modal parameters are very close and stable even at low numbers of averages. MAC values of above 0.9 also show good correlation of mode shapes between ISMA and EMA. The results are tabulated in Table 2.

Second mode and third mode are considered close to the running speed of 20 Hz as compared to first mode. The operating speed sat in between these two modes. Thus, slightly lower correlation is expected in this case. From Table 3 and Table 4, MAC values of second mode are below 0.9, ranging from 0.881 to 0.889 at different average settings, which indicate that there is a good correlation of mode shape between ISMA and benchmark i.e. EMA. The slight reduction in MAC values is due to the closeness of the second mode to operating speed at 20 Hz which contaminate the modal extraction of mode 2. Meanwhile, the third mode at 5 averages recorded low MAC value at 0.665. By increasing the average numbers, MAC value improved to 0.8 and consistency of the mode shape vectors between EMA and ISMA is established.

In short, when excitation frequency is far from any natural modes, ISMA with moderate number of averages taken could be used to extract the modal parameters even when the machines are running. Figures 3 to 6 show that increased number of impacts reduces the amplitude of unaccounted forces significantly. This is because by increasing average numbers, there are higher possibility to achieve differences in phases between responses due to cyclic loads, and responses due to impacts applied.

At 30 Hz, vibration level increased because of the amplified rotational or imbalance force,  $F=mr\omega^2$  where  $\omega$  is the rotational speed in rad/s. Since the first and second modes are far from the excitation frequency, modal parameters of these two modes were successfully extracted and well correlated with EMA. The results are as tabulated in Tables 2 and 3. MAC values around 0.95 also indicate high correlation of mode shape between ISMA and EMA.

On the other hand, high speed cyclic load and ambient excitation which are near to the third mode are dominant and they covered up the third mode. Responses of cyclic load are more significant than the responses generated by the impact. Figure 7 shows that for the first five impacts, the responses of excitation frequency are too large and they covered up the third mode. Therefore, third mode could not be determined. Table 4 shows that the natural frequency of third mode could be obtained by increasing the number of averages. In Figure 8, it shows that the responses generated by this cyclic load were greatly reduced after 250 impacts. Table 4 also shows that MAC improves from 0.713 to 0.763 when number of averages increase from 25 to 250. The mode shapes between EMA and ISMA achieve more than 75% correlation after 250 impacts.

When the machine is running at high frequency, ISMA with high number of impacts could successfully determine the dynamic characteristics. The extracted natural frequencies are well correlated. However, for natural modes that are close to the excitation frequency, mode shape correlation is considered slightly low due to dominant response of the excitation frequency as compared to impulse response. Therefore, besides average numbers, the amount of impact forces applied is another important parameter in performing ISMA. The amount of impact forces applied need to be re-calculated to overcome the force generated by cyclic load and ambient excitation at higher speeds. Excessive impacts may result in non-linearity and affect the accuracy of modal extractions. This will be the subject of future investigations. The results of the investigation on amount of impact forces applied in ISMA will be discussed in the authors' subsequent paper.

## **5. CONCLUSION**

This study has demonstrated the effectiveness of averages taken in the determination of dynamic characteristics of a machine while in different rotating speeds. The application of Impact-Synchronous Time

Averaging is effective in filtering out the non-synchronous running speed and its harmonics and noise at certain conditions. At low operating speeds which coincided with the lower natural modes, ISMA with high number of impacts applied successfully determined the dynamic characteristics of the system. Meanwhile, at operating speeds which were far from any natural modes, ISMA with moderate number of averages taken was sufficient to extract the modal parameters. Finally for high speed machines, ISMA with high number of impacts taken has limitation in extracting natural modes close to the operating speed. In order to rectify this problem, the amount of impact forces applied needs to be re-calculated so that it overcomes the force due to the cyclic load and ambient excitation at higher speed.

#### **ACKNOWLEDGEMENT**

The authors wish to acknowledge the financial support and advice given by Postgraduate Research Fund (PV086-2011A), Advanced Shock and Vibration Research (ASVR) Group of University of Malaya, and other project collaborators.

#### **REFERENCES**

- Allemang RJ. (2003) The modal assurance criterion - Twenty years of use and abuse. *Sound and Vibration* 37(8): 14-23.
- Avitabile P. (2011) Modal Space Back to Basics. *Experimental Techniques* 35(1): 1-2.
- Brincker R, Zhang LM and Anderson P. (2000) Modal Identification from Ambient Response using Frequency Domain Decomposition. *Proceedings of the 18th International Modal Analysis Conference*. San Antonio, Texas, USA, 625-630.

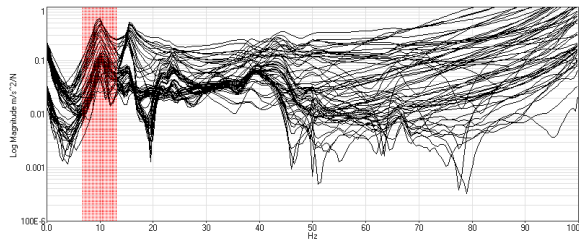
- Brown DL, Allemang RJ, Zimmerman R, et al. (1985) Parameter estimation techniques for modal analysis. *Seventh International Seminar on Modal Analysis*. Katholieke Universiteit Leuven, Leuven, Belgium.
- Fayyadh MM, Razak HA and Ismail Z. (2011) Combined modal parameters-based index for damage identification in a beamlike structure: theoretical development and verification. *Archives of Civil and Mechanical Engineering* 11(3): 587-609.
- Ibrahim SR and Mikulcik EC. (1973) A time domain vibration test technique. *The Shock and Vibration Bulletin* 43(4): 21–37.
- Ibrahim SR and Mikulcik EC. (1976) The experimental determination of vibration parameters from time responses. *The Shock and Vibration Bulletin* 46(5): 187–196.
- Ibrahim SR and Mikulcik EC. (1977) A method for direct identification of vibration parameters from the free response. *The Shock and Vibration Bulletin* 47(4): 183–198.
- Ismail Z. (2012) Application of residuals from regression of experimental mode shapes to locate multiple crack damage in a simply supported reinforced concrete beam. *Measurement* 45(6): 1455–1461.
- Ismail Z, Ong AZC and Rahman AGA. (2011) Crack damage detection of reinforced concrete beams using local stiffness indicator. *Scientific Research and Essays* 6(34): 6798-6803.
- Ismail Z and Ong ZC. (2012) Honeycomb damage detection in a reinforced concrete beam using frequency mode shape regression. *Measurement* 45(5): 950-959.
- James GH, Carne TG and Lauffer JP. (1995) The Natural Excitation Technique (Next) for Modal Parameter Extraction from Operating Structures. *Modal Analysis-the International Journal of Analytical and Experimental Modal Analysis* 10(4): 260-277.
- Juang JN and Pappa RS. (1985) An Eigensystem Realization-Algorithm for Modal Parameter-Identification and Model-Reduction. *Journal of Guidance Control and Dynamics* 8(5): 620-627.

- Kang D, Ming X and Xiaofei Z. (2000) Phase difference correction method for phase and frequency in spectral analysis. *Mechanical Systems and Signal Processing* 14(5): 835-843.
- Lardies J and Larbi N. (2001a) Dynamic system parameter identification by stochastic realization methods. *Journal of Vibration and Control* 7(5): 711-728.
- Lardies J and Larbi N. (2001b) Modal analysis of random vibrating systems from multi-output data. *Journal of Vibration and Control* 7(3): 339-363.
- Maia NMM and Silva JMM. (1997) *Theoretical and Experimental Modal Analysis*, Taunton, Somerset, UK: Research Studies Press.
- Ming X and Kang D. (1996) Corrections for frequency, amplitude and phase in a fast Fourier transform of a harmonic signal. *Mechanical Systems and Signal Processing* 10(2): 211-221.
- Mohanty P and Rixen DJ. (2004) A modified Ibrahim time domain algorithm for operational modal analysis including harmonic excitation. *Journal of Sound and Vibration* 275(1-2): 375-390.
- Ong ZC, Rahman AGA and Ismail Z. (2012) Determination of Damage Severity on Rotor Shaft Due to Crack Using Damage Index Derived From Experimental Modal Data. *Experimental Techniques: (In Press)*.
- Pappa RS and Ibrahim SR. (1981) A parametric study of the Ibrahim time domain modal identification algorithm. *The Shock and Vibration Bulletin* 51(3): 43-57.
- Qi KY, He ZJ, Li Z, et al. (2008) Vibration based operational modal analysis of rotor systems. *Measurement* 41(7): 810-816.
- Rahman AGA, Ong ZC and Ismail Z. (2011a) Effectiveness of Impact-Synchronous Time Averaging in determination of dynamic characteristics of a rotor dynamic system. *Measurement* 44(1): 34-45.
- Rahman AGA, Ong ZC and Ismail Z. (2011b) Enhancement of coherence functions using time signals in Modal Analysis. *Measurement* 44(10): 2112-2123.

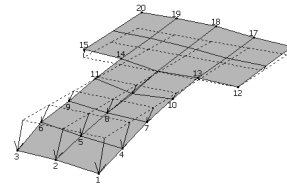
- Richardson MH and Formenti DL. (1982) Parameter Estimation from Frequency Response Measurements Using Rational Fraction Polynomials. *Proceedings of the 1st International Modal Analysis Conference*. Orlando, Florida, USA, 167–186.
- Richardson MH and Formenti DL. (1985) Global Curve Fitting of Frequency Response Measurements Using the Rational Fraction Polynomial Method. *Proceedings of the 3rd International Modal Analysis Conference*. Orlando, Florida, USA, 390–397.
- Schwarz B and Richardson MH. (2001) Modal Parameter Estimation from Ambient Response Data. *Proceedings of the 19th International Modal Analysis Conference*. Orlando, Florida, USA, 1017-1022.
- Schwarz B and Richardson MH. (2007) Using a De-Convolution Window for Operating Modal Analysis. *Proceedings of the 2nd International Operational Modal Analysis Conference*. Orlando, Florida, USA, 1-7.
- Shih CY, Tsuei YG, Allemang RJ, et al. (1988) A Frequency-Domain Global Parameter-Estimation Method for Multiple Reference Frequency-Response Measurements. *Mechanical Systems and Signal Processing* 2(4): 349-365.
- Whelan MJ, Gangone MV, Janoyan KD, et al. (2011) Operational modal analysis of a multi-span skew bridge using real-time wireless sensor networks. *Journal of Vibration and Control* 17(13): 1952-1963.
- Zhang LM, Brincker R and Andersen P. (2001) Modal Indicators for Operational Modal Identification. *Proceedings of the 19th International Modal Analysis Conference*. Orlando, Florida, USA, 746-752.

Table 1

Mode 1



3DView: 10.1 Hz [Max]



Ampl: 1.0, Dwell: 10  
Persp: +10



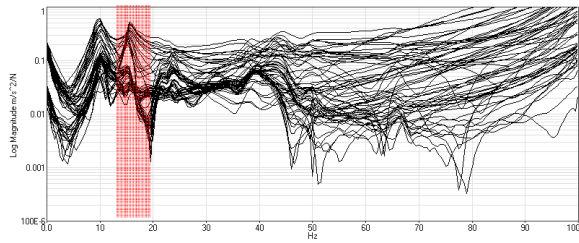
Natural Frequency (Hz)

9.92

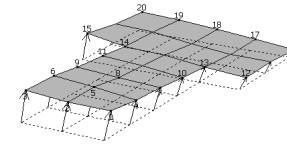
Damping ratio (Hz)

1.020

Mode 2



3DView: 15.4 Hz [Max]



Ampl: 1.0, Dwell: 10  
Persp: +10



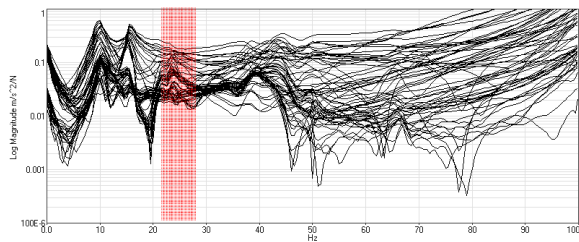
Natural Frequency (Hz)

15.60

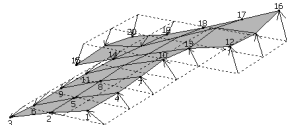
Damping ratio (Hz)

0.676

Mode 3



3DView: 23.6 Hz [Max]



Ampl: 1.0, Dwell: 10  
Persp: +10



Natural Frequency (Hz)

24.90

Damping ratio (Hz)

0.888

Table 2

<b>Mode 1</b>	<b>Natural Frequency (Hz)</b>	<b>Damping (Hz)</b>	<b>MAC</b>
<b>Static 5 Averages</b>	9.92	1.020	-
<b>Running at 10Hz 5 Averages</b>	9.81	0.659	0.718
<b>Running at 10Hz 25 Averages</b>	9.62	0.880	0.892
<b>Running at 10Hz 50 Averages</b>	9.59	0.871	0.932
<b>Running at 10Hz 100 Averages</b>	9.56	0.901	0.957
<b>Running at 10Hz 150 Averages</b>	9.56	0.903	0.957
<b>Running at 10Hz 200 Averages</b>	9.55	0.901	0.951
<b>Running at 10Hz 250 Averages</b>	9.58	0.863	0.953
<b>Running at 20Hz 5 Averages</b>	9.58	0.885	0.948
<b>Running at 20Hz 25 Averages</b>	9.58	0.891	0.953
<b>Running at 20Hz 50 Averages</b>	9.57	0.889	0.961
<b>Running at 20Hz 100 Averages</b>	9.56	0.886	0.958
<b>Running at 20Hz 150 Averages</b>	9.55	0.885	0.956
<b>Running at 20Hz 200 Averages</b>	9.55	0.885	0.952
<b>Running at 20Hz 250 Averages</b>	9.59	0.858	0.953
<b>Running at 30Hz 5 Averages</b>	9.51	0.908	0.971
<b>Running at 30Hz 25 Averages</b>	9.52	0.912	0.962
<b>Running at 30Hz 50 Averages</b>	9.51	0.910	0.962
<b>Running at 30Hz 100 Averages</b>	9.51	0.908	0.963
<b>Running at 30Hz 150 Averages</b>	9.51	0.909	0.963
<b>Running at 30Hz 200 Averages</b>	9.51	0.909	0.961
<b>Running at 30Hz 250 Averages</b>	9.57	0.877	0.955

Table 3

<b>Mode 2</b>	<b>Natural Frequency (Hz)</b>	<b>Damping (Hz)</b>	<b>MAC</b>
<b>Static 5 Averages</b>	15.60	0.676	-
<b>Running at 10Hz 5 Averages</b>	15.20	0.723	0.915
<b>Running at 10Hz 25 Averages</b>	15.20	0.724	0.909
<b>Running at 10Hz 50 Averages</b>	15.20	0.725	0.911
<b>Running at 10Hz 100 Averages</b>	15.20	0.726	0.911
<b>Running at 10Hz 150 Averages</b>	15.20	0.726	0.911
<b>Running at 10Hz 200 Averages</b>	15.20	0.726	0.910
<b>Running at 10Hz 250 Averages</b>	15.20	0.726	0.910
<b>Running at 20Hz 5 Averages</b>	15.20	0.680	0.883
<b>Running at 20Hz 25 Averages</b>	15.20	0.679	0.884
<b>Running at 20Hz 50 Averages</b>	15.20	0.678	0.886
<b>Running at 20Hz 100 Averages</b>	15.20	0.678	0.889
<b>Running at 20Hz 150 Averages</b>	15.20	0.678	0.886
<b>Running at 20Hz 200 Averages</b>	15.20	0.679	0.881
<b>Running at 20Hz 250 Averages</b>	15.20	0.697	0.883
<b>Running at 30Hz 5 Averages</b>	15.20	0.686	0.923
<b>Running at 30Hz 25 Averages</b>	15.20	0.692	0.937
<b>Running at 30Hz 50 Averages</b>	15.20	0.694	0.941
<b>Running at 30Hz 100 Averages</b>	15.20	0.695	0.948
<b>Running at 30Hz 150 Averages</b>	15.20	0.694	0.949
<b>Running at 30Hz 200 Averages</b>	15.20	0.693	0.950
<b>Running at 30Hz 250 Averages</b>	15.20	0.693	0.949

Table 4

<b>Mode 3</b>	<b>Natural Frequency (Hz)</b>	<b>Damping (Hz)</b>	<b>MAC</b>
<b>Static 5 Averages</b>	24.90	0.888	-
<b>Running at 10Hz 5 Averages</b>	23.40	0.992	0.784
<b>Running at 10Hz 25 Averages</b>	23.40	0.954	0.803
<b>Running at 10Hz 50 Averages</b>	23.40	0.945	0.818
<b>Running at 10Hz 100 Averages</b>	23.40	0.953	0.858
<b>Running at 10Hz 150 Averages</b>	23.50	0.954	0.865
<b>Running at 10Hz 200 Averages</b>	23.50	0.952	0.868
<b>Running at 10Hz 250 Averages</b>	23.50	0.955	0.871
<b>Running at 20Hz 5 Averages</b>	23.20	1.150	0.665
<b>Running at 20Hz 25 Averages</b>	23.20	1.290	0.812
<b>Running at 20Hz 50 Averages</b>	23.40	1.260	0.825
<b>Running at 20Hz 100 Averages</b>	23.40	1.290	0.809
<b>Running at 20Hz 150 Averages</b>	23.40	1.300	0.813
<b>Running at 20Hz 200 Averages</b>	23.40	1.300	0.813
<b>Running at 20Hz 250 Averages</b>	23.30	1.320	0.820
<b>Running at 30Hz 5 Averages</b>	N/A	N/A	N/A
<b>Running at 30Hz 25 Averages</b>	23.60	1.200	0.712
<b>Running at 30Hz 50 Averages</b>	23.60	1.120	0.722
<b>Running at 30Hz 100 Averages</b>	23.70	1.220	0.722
<b>Running at 30Hz 150 Averages</b>	23.70	1.250	0.731
<b>Running at 30Hz 200 Averages</b>	23.60	1.180	0.752
<b>Running at 30Hz 250 Averages</b>	23.60	1.220	0.763

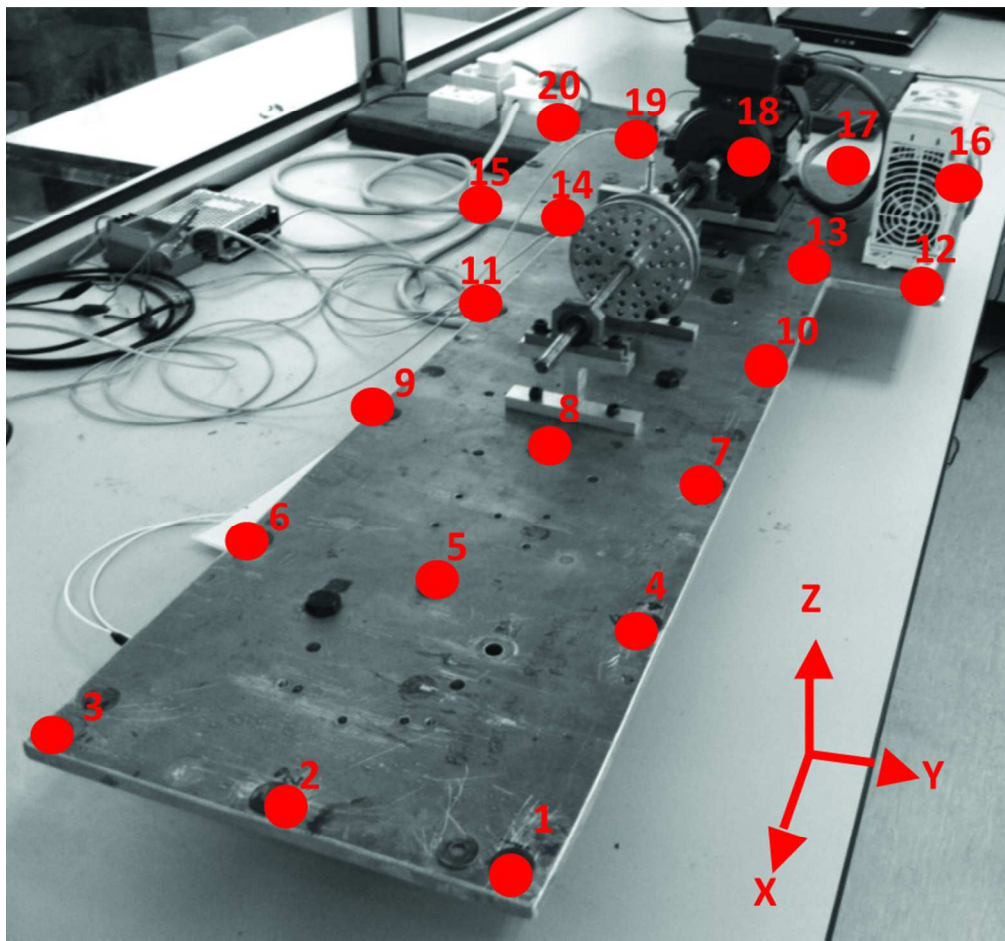


Fig. 1: Fault Simulation Rig  
81x76mm (300 x 300 DPI)

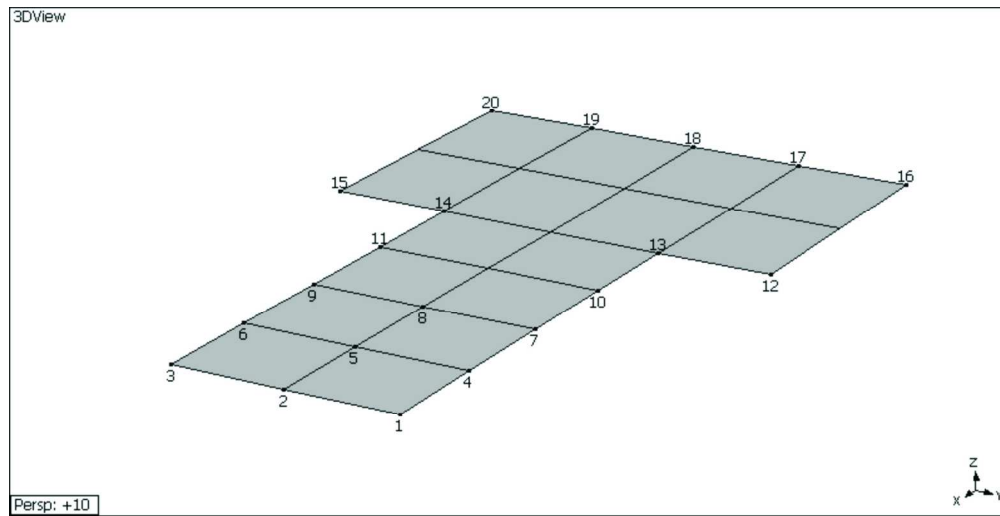


Fig. 2: Structural model of the Fault Simulation Rig  
149x76mm (300 x 300 DPI)

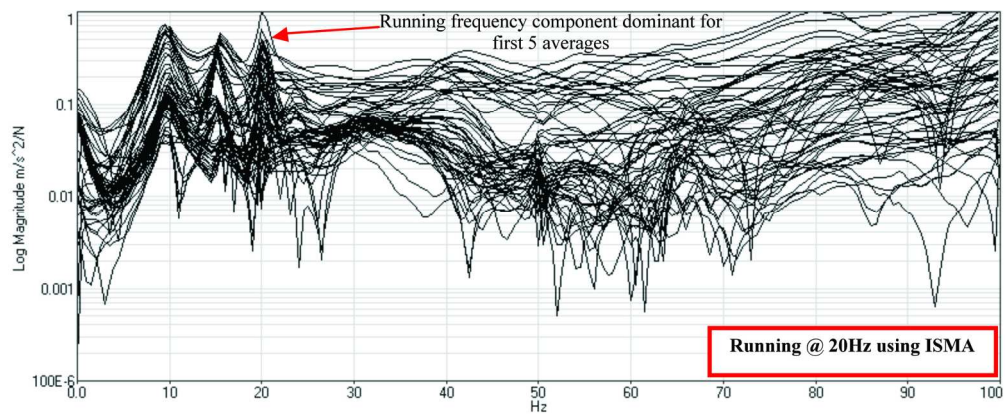


Fig. 3: Overlaid ISMA FRFs running at 20Hz with 5 averages  
165x66mm (300 x 300 DPI)

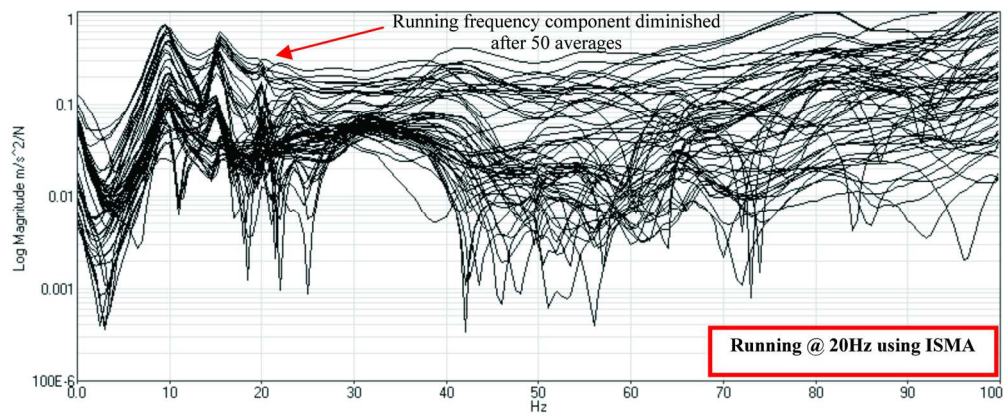


Fig. 4: Overlaid ISMA FRFs running at 20Hz with 50 averages  
165x66mm (300 x 300 DPI)

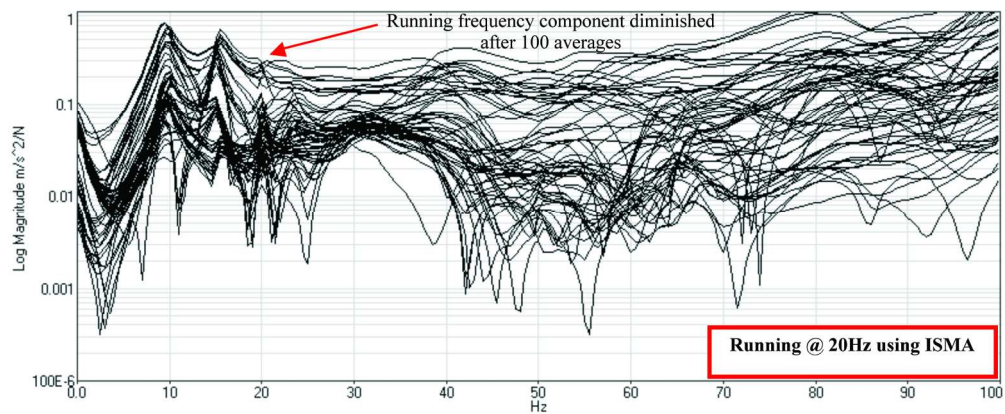


Fig. 5: Overlaid ISMA FRFs running at 20Hz with 100 averages  
165x66mm (300 x 300 DPI)

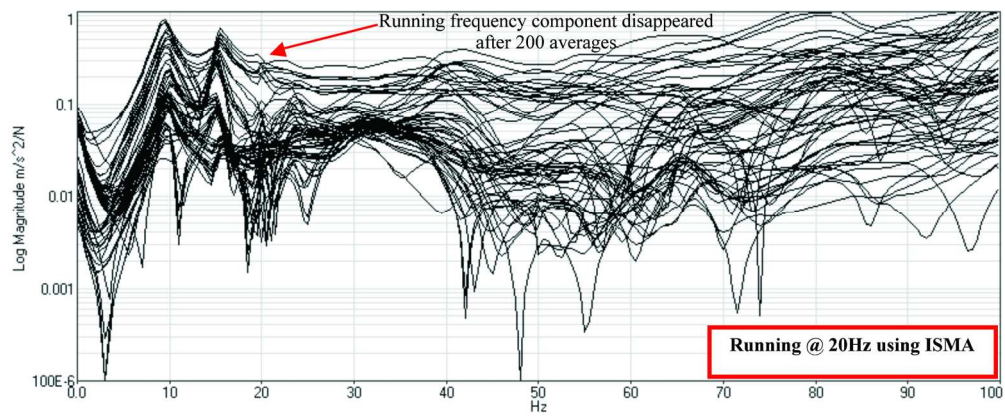


Fig. 6: Overlaid ISMA FRFs running at 20Hz with 200 averages  
165x66mm (300 x 300 DPI)

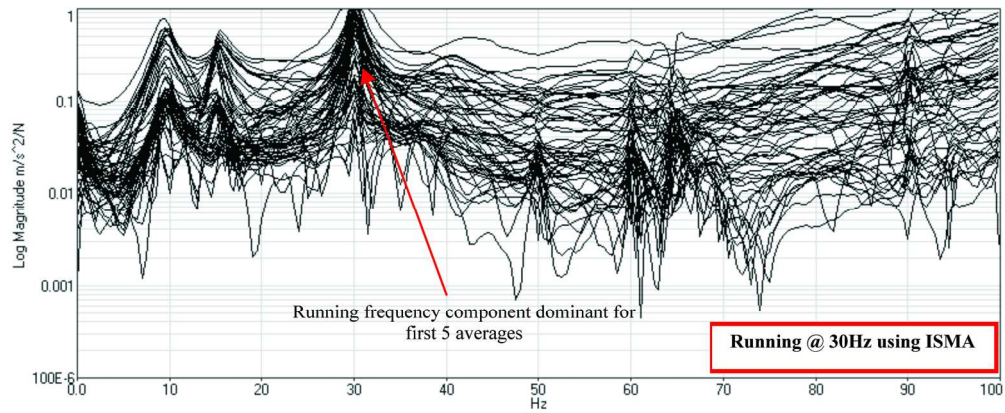


Fig. 7: Overlaid ISMA FRFs running at 30Hz with 5 averages  
165x66mm (300 x 300 DPI)

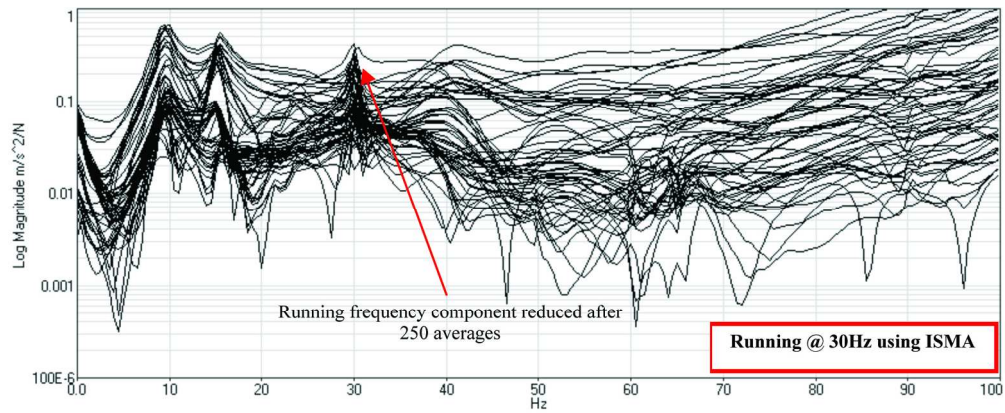


Fig. 8: Overlaid ISMA FRFs running at 30Hz with 250 averages  
165x66mm (300 x 300 DPI)

## List of Table and Figure Captions

Table 1: Dynamic characteristics of fault simulation rig during static condition	Page 8
Table 2: Comparison of dynamic characteristics of 1 <sup>st</sup> mode at different operating speeds and averages	Page 9
Table 3: Comparison of dynamic characteristics of 2 <sup>nd</sup> mode at different operating speeds and averages	Page 9
Table 4: Comparison of dynamic characteristics of 3 <sup>rd</sup> mode at different operating speeds and averages	Page 10
Fig. 1: Fault Simulation Rig	Page 7
Fig. 2: Structural model of the Fault Simulation Rig	Page 8
Fig. 3: Overlaid ISMA FRFs running at 20Hz with 5 averages	Page 11
Fig. 4: Overlaid ISMA FRFs running at 20Hz with 50 averages	Page 11
Fig. 5: Overlaid ISMA FRFs running at 20Hz with 100 averages	Page 11
Fig. 6: Overlaid ISMA FRFs running at 20Hz with 200 averages	Page 11
Fig. 7: Overlaid ISMA FRFs running at 30Hz with 5 averages	Page 11
Fig. 8: Overlaid ISMA FRFs running at 30Hz with 250 averages	Page 11